Cross polarization in microwave antennas: Case study of a circular waveguide

Polarización cruzada en antenas de microondas: Caso de estudio de una guía de onda circular

Daniel Santillán-Haro [1,2]*, Eva Antonino-Daviu [2], Miguel Ferrando Bataller [2], Daniel Sánchez-Escuderos [2], Diana Navarro-Méndez [3], Fernando Carrera-Suárez [3]

[1]*Facultad de Ingeniería, Universidad Nacional de Chimborazo, Riobamba, Ecuador*

[2]*Instituto de Telecomunicaciones y Aplicaciones Multimedia, Universitat Politècnica de València, Valencia, Spain; evanda@upvnet.upv.es; mferrand@dcom.upv.es; dasanes1@gmail.com*

[3]*Escuela Politécnica Nacional, Quito, Ecuador; veronica.navarro@epn.edu.ec; fernando.carrera@epn.edu.ec*

* Correspondence: dsantillan@unach.edu.ec

Abstract: During the last decade, the subject of antenna polarization attracts great interest. The improve of the cross polarization generates a distribution of a highly symmetric field in the aperture of the antenna, however, it is difficult to make low cross polarization circular sources to operate over a wide bandwidth. In this paper, a study case is presented to improve the cross polarization of a circular aperture. As the circular waveguide has a poor cross polarization, three possible solutions have been considered to improve the cross polarization in previous works. The first solution is based on a metallic disk, which after an optimization process obtains an external diameter of 90.42mm. The second solution is based on a metallic ring around the circular waveguide, the optimized dimension of the external diameter ring is 90.42mm with a thickness of 1.63mm. The third solution is based on two rings around the circular waveguide, which optimized dimensions of the rings are an outer diameter of 122.48mm, and an inner diameter of 90.42mm. This knowledge is valuable to explain the improvement of matching level of a patch antenna with a ring around 5.8 GHz.

Keywords: Circular polarization, cross polarization, metallic rings, numerical analysis, patch antenna.

Resumen: *Durante la última década, el tema de la polarización de la antena atrae gran interés. La mejora de la polarización cruzada genera una distribución de un campo altamente simétrico en la apertura de una antena, sin embargo, es difícil hacer fuentes circulares de baja polarización cruzada que operen en un ancho de banda amplio. En este artículo se presenta un caso de estudio para mejorar la polarización cruzada de una apertura circular. Como la guía de onda circular tiene una polarización cruzada pobre, se han considerado tres soluciones posibles para mejorar la polarización cruzada, que ha sido presentada en trabajos anteriores. La primera solución se basa en un disco metálico que, después de un proceso de optimización, se obtiene un diámetro externo optimizado de 90.42 mm. La segunda solución se basa en un anillo metálico alrededor de la guía de onda circular, la dimensión optimizada del anillo de diámetro externo es de 90.42 mm con un grosor de 1.63 mm. La tercera solución se basa en dos anillos alrededor de la guía de onda circular, cuyas dimensiones optimizadas son un diámetro exterior de 122.48 mm y un diámetro interno de 90.42 mm. El conocimiento obtenido es valioso para explicar la mejora del nivel de adaptación de una antena de parche con un anillo de alrededor a 5.8 GHz.*

Palabras clave: *Polarización circular, polarización cruzada, anillos metálicos, análisis numérico, antena de parche.*

1 Introduction

For more than a decade, the subject of antenna polarization has generated great interest. The definition can be complex as radiating and receiving structures respond differently, both in frequency and angle between the incident and transmitted wave (Thornton & Huang, 2013). When antenna patterns are taken in the usual way, the Ludwig definition is commonly used. In (Ludwig, 1973) the definitions of co-polarization (reference polarization), and cross polarization applied to linearly polarized antennas are presented. An antenna radiation in a specified polarization, which is called reference polarization; whereas radiation in the orthogonal polarization is known as cross-polarization (Aznar *et al.*, 2004). In addition, Ludwig's definitions are clarified using different polarized reference sources located linearly in different orientations (Aboserwal *et al.*, 2018). The low cross polarization generates a distribution of a highly symmetric field in the aperture, however, it is difficult to achieve a reduction of cross polarization over a wide bandwidth.

Alternatively, a wideband approach for significantly reducing the cross-polarization levels of standard-gain horns, for an X-band standard from 6.5 GHz to 18 GHz, applying filter screens has been proposed (Kuloglu & Chen, 2013). In addition, to improve the cross-polarization performance, two pairs of arc-shaped slots have been added to the ring slot antenna, for a circular aperture antenna with differential feeding (Chen *et al.*, 2017). Also, a defected ground structure with integrated square patch has been proposed (Kumar *et al.*, 2015). The defect is deployed surrounding the element maintaining a considerable spacing from the patch boundary. Moreover, the undesired cross polarization of the reflector antennas, can be reduced with a circular-rim (Pour & Shafai, 2012). In this paper, we propose the analysis and simulation of a circular waveguide with the addition of metallic rings as elements to improve the radiation pattern in the $3-7$ GHz band. The simulation of the antenna has been done with a CST frequency domain solver (Dassault Systemes, 2018). Finally, to validate the concept, metallic square rings are added in the design of a patch antenna at 5.8 GHz.

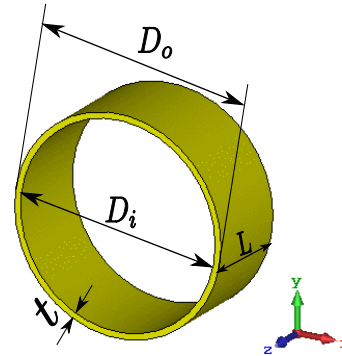# 2 Modeling a circular waveguide with metallic rings

Figure 1: Geometry of the circular waveguide.

2.1 Circular waveguide

The main parameters of a circular waveguide are the length of the enclosing metallic wall (L), and the inner diameter of the circular waveguide (D_i). The thickness of the waveguide (t) does not affect the bandwidth, therefore a standard waveguide WR-229 can be used, which thickness is 1.63 mm.

The cutoff frequency of the circular waveguide is determined by the equations (1) y (2) (Balanis, 2012), where ρ is the radius of the waveguide, χ_{mn} are the roots of Bessel functions and χ'_{mn} are the roots of the derivative of the Bessel functions.

$$f_c|TE_{mn} = \frac{1}{2\pi\sqrt{\mu\varepsilon}}\frac{\chi'_{mn}}{\rho} \qquad (1)$$

$$f_c|TM_{mn} = \frac{1}{2\pi\sqrt{\mu\varepsilon}}\frac{\chi_{mn}}{\rho} \qquad (2)$$

Taking into account that the waveguide is modeled as PEC (perfectly electrical conductor), the dominant circular waveguide mode is TE_{11} (Pozar, 2009), and the following mode is TM_{01}. The cutoff frequencies of these modes can be obtained with equations (1) and (2).

For a cutoff frequency of 3.25 GHz for mode TE_{11}, it can be deduced from (1) that the radius of the waveguide must be $\rho = 27.03$ mm. Table 1, shows the values of the cutoff frequencies for the different modes of the circular waveguide with this radius. The geometry of the circular waveguide is depicted in figure 1, with an inner diameter $D_i = 54.06$ mm (0.65 λ), an external diameter $D_o = 57.32$ mm (0.69 λ), and a length $L = 25$ mm, where λ is the free-space wavelength at the design frequency ($f = 3.625$ GHz).

To validate the performance of the circular waveguide, the S_{11} parameter is simulated. As can be ob-

Table 1: Modes of a circular waveguide.

Modo	$f/f_c|TE_{11}$	F(GHz)
TE_{11}	1	3.25
TM_{01}	1.3	4.245
TE_{21}	1.66	5.395
TE_{01}	2.08	6.76
TM_{11}	2.08	6.76
TE_{31}	2.28	7.41
TM_{21}	2.79	9.07
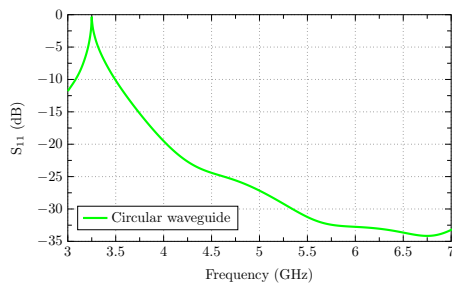
Figure 2: Simulated S_{11} parameter of the circular waveguide.
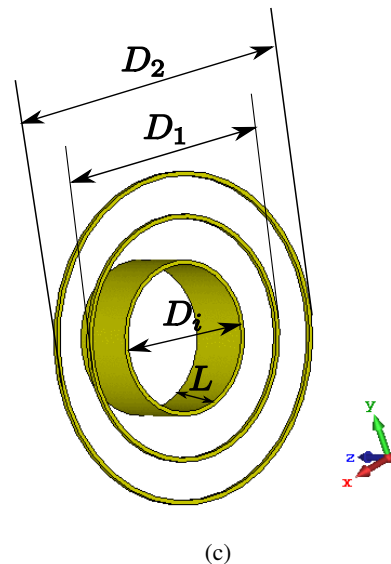

(a)

(b)

(c)

Figure 3: Proposed solutions to improve cross polarization in a circular waveguide. (a) Metallic disk. (b) Metallic ring. (c) Two metallic rings.

served in figure 2, the result show a good matching ($S_{11} < -10$ dB) from 3.5 to 7 GHz.

2.2 Analysis with metallic rings

As the circular waveguide has a poor cross polarization, three possible solutions have been considered to improve the cross polarization (Santillan, 2017). The first solution is to add a metallic disk as shown in figure 3(a). After an optimization process the value of the external diameter is $D_1 = 90.42$ mm.

The second solution is to place a metallic ring around the circular waveguide (see figure 3(b)). The optimized dimension of the external diameter ring is $D_1 = 90.42$ mm with a thickness of 1.63 mm.

A third solution is to place 2 rings around the circular waveguide as indicated in figure 3(c). The optimized dimensions of the rings are: an outer diameter of $D_2 = 122.48$ mm, and an inner Diameter $D_1 = 90.42$ mm. Note that the thickness of the rings has the same value as the second solution.
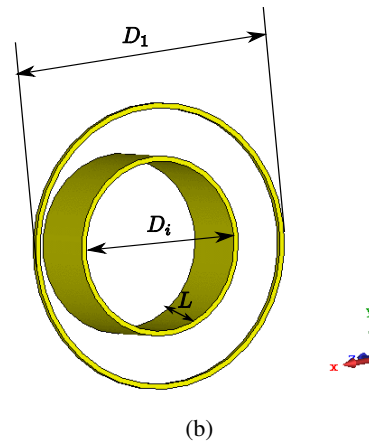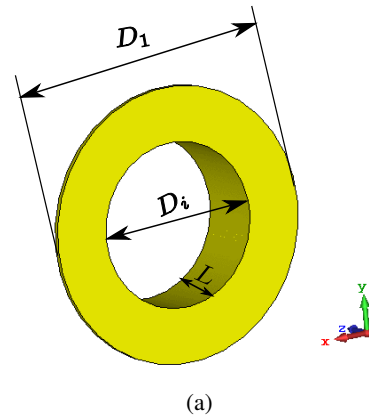
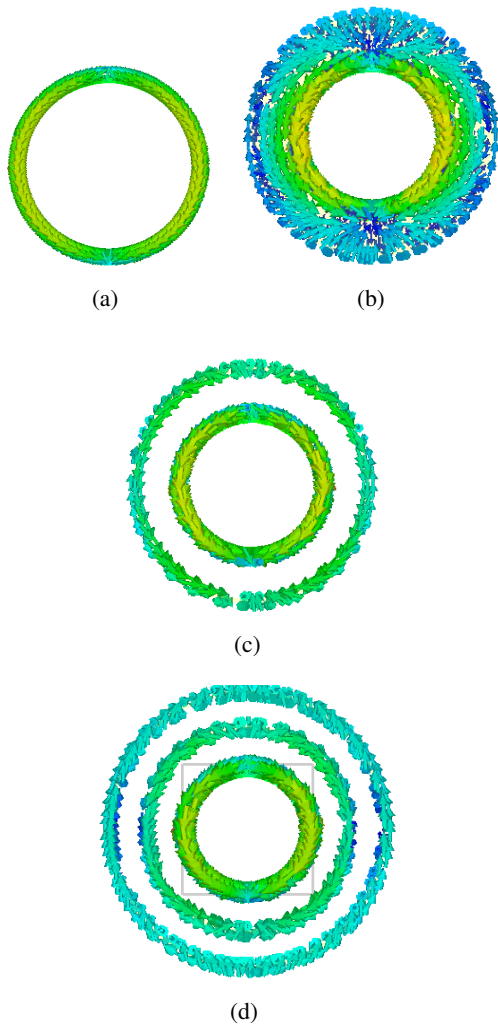(a)   (b)

(c)

(d)

Figure 4: Surface current distribution at the design frequency ($f = 3.625$ GHz). (a) Circular waveguide. (b) Metallic disk. (c) Metallic ring. (d) Two metallic rings.

3   Simulated results and validation with a patch antenna

Figure 4 shows the surface current distributions of the proposed solutions. It is clear that the currents are concentrated around the internal diameter D_i of the metallic disk (see figure 4(b)). Figs. 4(c) and 4(d) show the total current in one and two rings, respectively. Observe that the distribution of the current in the circular waveguide is the same as in the metallic ring, while in the configuration of two rings, the current densities have the same direction in the internal radius, and in the outer radius the
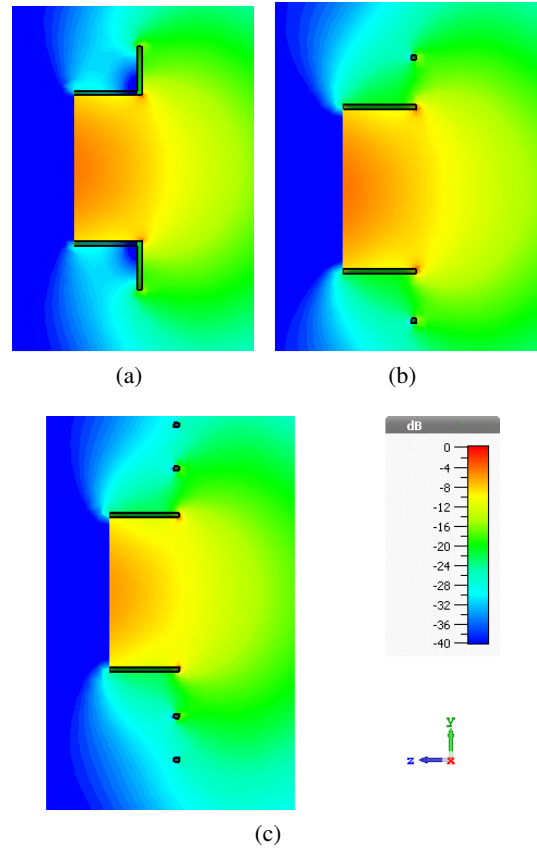

(a)   (b)

(c)

Figure 5: Electric Field distribution at the design frequency ($f = 3.625$ GHz) of the circular waveguide. (a) Metallic disk. (b) Metallic ring. (c) Two metallic rings.
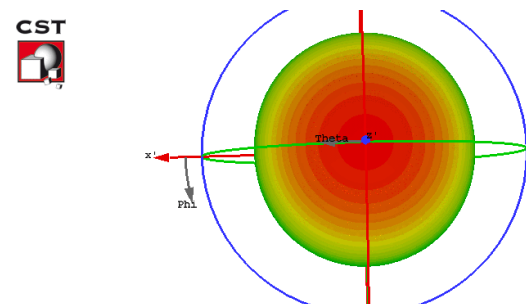

Figure 6: Simulation of the radiation pattern of the proposed configuration at 3.625 GHz.

currents are opposite and small. In figure 5, the simulated E-field distribution of the circular waveguide with metallic rings is presented. As can be observed, the electric field distribution in the metallic rings is symmetric, which gives an improvement in the radiation diagram (figure 6).
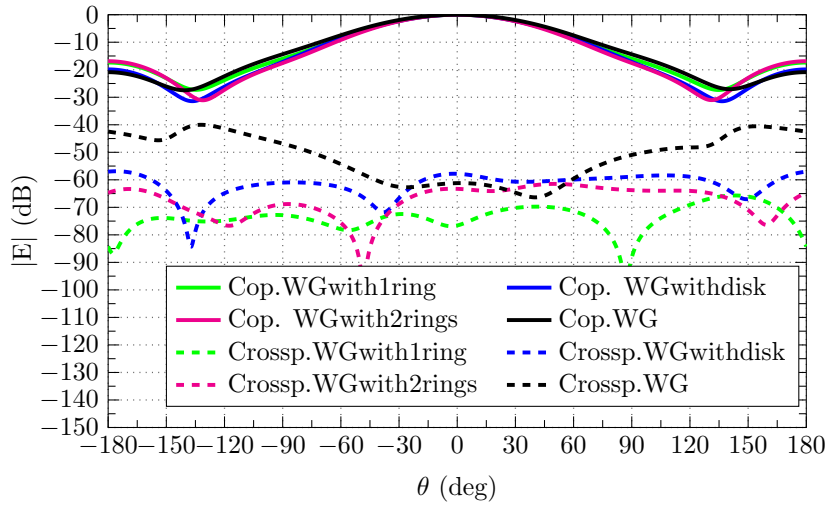
Figure 7: Copolar (Cop.) and cross-polar (Crossp) components of the radiation pattern in the xz plane at 3.625 GHz for the proposed configurations.
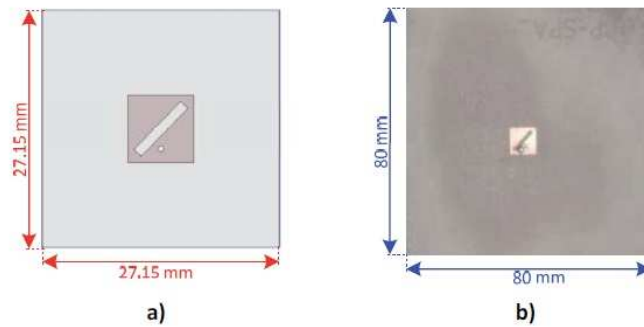

Figure 8: Path antenna. (a) Simulated with HFSS. (b) Large antenna built (Méndez, 2015).
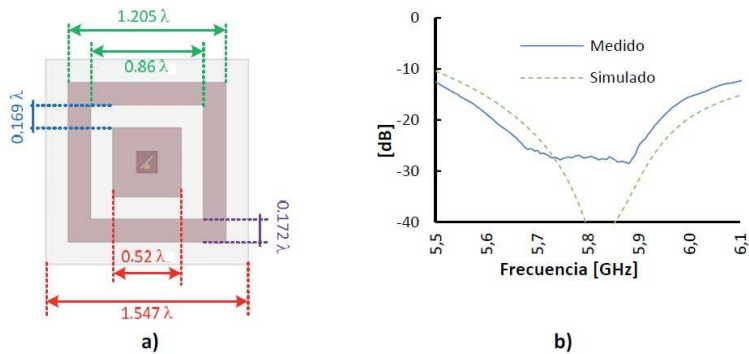

Figure 9: Modified path antenna. (a) Scheme. (b) S_{11} parameter (Méndez, 2015).
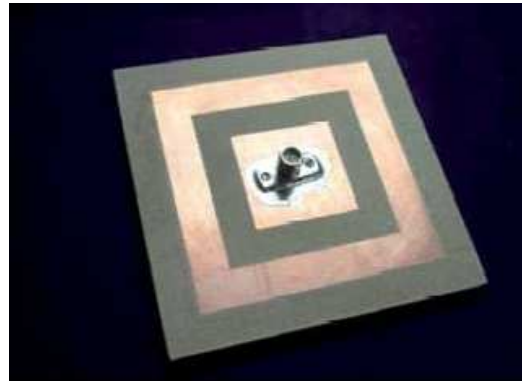
Figure 10: Prototype of the patch antenna with a square metallic ring around it (Méndez, 2015).
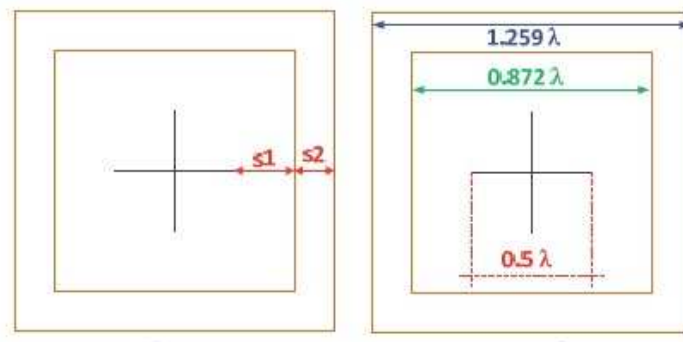

Figure 11: Electrical dimensions of the patch antenna with two metallic rings (Méndez *et al.*, 2013).
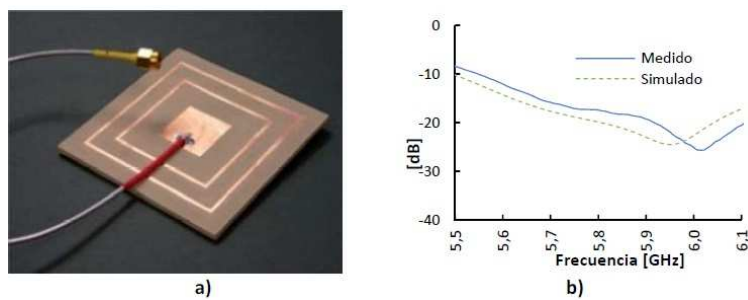

Figure 12: Picture of the antenna with two square metallic rings (Méndez *et al.*, 2013).

Figure 7 shows the copolar and cross−polar components of the radiation pattern on the xz−plane at 3.625 GHz. As it can be seen, the cross-polar component is 50 dB below the copolar component within the main beam.

3.1 Patch antenna with a surrounding metallic ring

A patch antenna type is the thinnest element for circular polarization (Méndez, 2015). For implementation it is considered an antenna with dimensions as shown in figure 8.

The results of the large antenna have a great similarity but increasing the size adversely affects the behavior of the diagram and polarization, so it is necessary to redesign.

3.1.1 Design modifications in the path antenna

Considering that electromagnetic band gap (EBG) structures are used to suppress the effects of surface waves (Cho & Lee, 2010), a metallic ring surrounding the original small ground plane is inserted, as can be seen in figure 9. The behavior of this square ring is similar to the one presented previously for circular rings. By varying the width of the metallic ring, and the distance from the plane, a good matching level is obtained (see figure 9 (b)).

A prototype of the path antenna with a surrounding metallic ring was fabricated and measured. A picture of the fabricated patch antenna is shown in figure 10.

As a second improvement, the ring thickness of figure 10 is replaced by another 2 thinner rings. The new dimensions are shown in figure 11. With the variables S_1 and S_2 we can tune the resonance frequency. If the spacing between the inner ring and dipoles is less than 0.20λ there is a frequency shift of 1% (approximately). For values of S_1 of 0.40 λ the bandwidth is increased by about 10% compared to the bandwidth of the dipoles without rings.

To improve the matching level, a circular groove (3 mm of diameter and 0.2 mm of width) located in the ground plane around the inner conductor can be introduced. The manufactured antenna with two surrounding metallic rings is shown in figure 12 (a). By replacing the large ring by 2 thinner rings, a bandwidth of 7.6% was obtained. In addition, a good matching level (S_{11} <-20dB) in the whole $5.5 - 6.10$ GHz band (see figure 12 (b)) was obtained.

4 Conclusion

In this work, the improvement of cross polarization were obtained through metallic rings around a microwave antenna. An open-ended circular waveguide was used as the primary feed for the metallic rings. The simulated structures provide a good cross-polar level (better than -50 dB) with a good matching level ($S_{11} < -14$ dB) from 3.5 to 7 GHz. To verify the design, a patch antenna with surrounding metallic rings was presented. Measured results show an optimum coupling, within a wide range of frequencies from 5.5 to 6.10 GHz.

Interest Conflict

The authors declare that they have no conflicts of interest.

Acknowledgment

References

Aboserwal, N. A., Salazar, J. L., Ortiz, J. A., Díaz, J. D., Fulton, C., & Palmer, R. D. (2018). Source current polarization impact on the cross polarization definition of practical antenna elements: Theory and applications. *IEEE Transactions on Antennas and Propagation*, 66(9), 4391–4406.

Aznar, Á., Robert, J., Casals, J., Roca, L., Boris, S., & Bataller, M. (2004). *Antenas*. Spain: Universidad Politécnica de Catalunya. Iniciativa Digital Politécnica.

Balanis, C. A. (2012). *Advanced engineering electromagnetics*. New York: John Wiley & Sons.

Chen, C., Li, C., Zhu, Z., & Wu, W. (2017). Wideband and low cross polarization planar annual ring slot antenna. *IEEE Antennas and Wireless Propagation Letters*, 16, 3009–3013.

Cho, T. & Lee, H. (2010). *Dual-band surface wave suppression using soft surface structure*. Paper presented at Antennas and Propagation (EuCAP), 2010 Proceedings of the Fourth European Conference, Retrieved from https://ieeexplore.ieee.org/.

Dassault Systemes (2018). CST Microwave Studio. https://www.cst.com.

Kuloglu, M. & Chen, C.-C. (2013). Ultra-wideband electromagnetic-polarization filter applications to conventional horn antennas for substantial cross-polarization level reductions. *IEEE Antennas and Propagation Magazine*, *55*(2), 280–288.

Kumar, C., Pasha, M. I., & Guha, D. (2015). Microstrip patch with nonproximal symmetric defected ground structure (dgs) for improved cross-polarization properties over principal radiation planes. *IEEE Antennas and Wireless Propagation Letters*, *14*, 1412–1414.

Ludwig, A. (1973). The definition of cross polarization. *IEEE Transactions on Antennas and Propagation*, *21*(1), 116–119.

Méndez, D. V. N. (2015). *Nuevos sistemas radiantes realizados con tecnologías impresas*. PhD thesis, Editorial Universitat Politècnica de València.

Méndez, D. V. N., Suárez, L. F. C., & Escudero, M. B. Circular polarization patch antenna with low axial ratio in a large beamwidth. In *Antennas and Propagation (EuCAP), 2013 7th European Conference on*, pp. 3330–3333. IEEE.

Pour, Z. A. & Shafai, L. (2012). A simplified feed model for investigating the cross polarization reduction in circular-and elliptical-rim offset reflector antennas. *IEEE Transactions on Antennas and Propagation*, *60*(3), 1261–1268.

Pozar, D. M. (2009). *Microwave Engineering*. New York: John Wiley & Sons.

Santillan, D. (2017). *Theses: Diseño de antenas directivas de banda ancha a frecuencias de microondas*. Universitat Politècnica de València.

Thornton, J. & Huang, K.-C. (2013). *Modern lens antennas for communications engineering*, volume 39. USA: John Wiley & Sons.